

Visualizing Two Qubits

J. E. Avron, G. Bisker and O. Kenneth

Department of Physics
Technion, 32000 Haifa, Israel

February 5, 2008

Abstract

The notions of entanglement witnesses, separable and entangled states for two qubits system can be visualized in three dimensions using the SLOCC equivalence classes. This visualization preserves the duality relations between the various sets and allows us to give “proof by inspection” of a non-elementary result of the Horodeckies that for two qubits, Peres separability test is iff. We then show that the CHSH Bell inequalities can be visualized as circles and cylinders in the same diagram. This allows us to give a geometric proof of yet another result of the Horodeckies, which optimizes the violation of the CHSH Bell inequality. Finally, we give numerical evidence that, remarkably, allowing Alice and Bob to use three rather than two measurements each, does not help them to distinguish any new entangled SLOCC equivalence class beyond the CHSH class.

1 Introduction

The world of 2 qubits is the simplest setting where the notions of entanglement [12, 4, 16], Bell inequalities [17, 19] and their witnesses [10], first appear. It would be nice if, like the Bloch sphere for one qubit [16], they could also be visualized geometrically. However, the world of two qubits is represented by 4×4 Hermitian matrices and being 16 dimensional it is not readily visualized. It can, however, be visualized by introducing an appropriate equivalence relation. This idea has been used in [15] to describe the separable and entangled

states. Here we show that the entanglement witnesses and the CHSH Bell inequalities can be incorporated in this descriptions as well. The geometric description is faithful to the duality between separable states and witnesses as we shall explain. This allows for elementary and elegant proofs of non-elementary results.

Any 4×4 hermitian operator W can be represented by a 4×4 real matrix ω using the Pauli matrices as the basis:

$$W = \omega_{\mu\nu} \sigma^\mu \otimes \sigma^\nu \quad (1.1)$$

Greek indices run on $0, 1, 2, 3$, Roman indices on $1, 2, 3$. σ^0 is the identity and σ^j are the Pauli matrices. Summation over a pair of repeated indices is always implied, and indices are raised and lowered using the Minkowski metric tensor $\eta = \text{diag}(1, -1, -1, -1)$. To reduce the number of components from 16 to 3 one relies on notions of equivalence. In particular, forgetting about the overall normalization of operators reduces the dimension by 1.

An effective notion of equivalence comes from allowing Alice and Bob to operate on their respective qubits

$$\rho \rightarrow \rho^M = M \rho M^\dagger, \quad M = A \otimes B, \quad (1.2)$$

We shall focus on the case $A, B \in SL(2, \mathbb{C})$ where the operation is invertible but not trace preserving. The physical interpretation of this is that states which are accessible by local, reversible filtering are identified. It is known as SLOCC [2, 8] and is briefly reviewed in section 2. Since $\dim SL(2, \mathbb{C}) = 6$ the SLOCC equivalence reduces the dimension by 12. As a consequence, the SLOCC equivalence classes of unnormalized 2 qubits states can be visualized in 3 dimensions.

As we shall see, the SLOCC equivalence classes of entanglement witnesses are represented by the cube, the states by the tetrahedron and the separable states by the octahedron of Fig. 1. The octahedron and tetrahedron have been identified as the SLOCC representation in [15, 26]. Adding the cube as a representation of the SLOCC equivalence classes of entanglement witnesses, shows that the natural duality relation between witnesses and separable states is preserved in the visualization of the SLOCC equivalence classes: The cube is the dual of the octahedron in the usual sense of duality of convex sets [20]. In particular, the number of faces in one is the number of vertices in the other. The tetrahedron is, of course, its own dual.

Since the work of the Horodeckis, [13], Fig. 1 has been widely used in quantum information theory for the special cases of states with maximally mixed subsystems [3, 27]. This is a 9 dimensional family of states with $\omega_{0j} = \omega_{j0} = 0$ in Eq. (1.1). Since this family has lower dimension, it can be visualized in 3 dimensions using a more restrictive notion of equivalence than SLOCC: Alice and Bob are allowed to perform only unitary operations on their respective qubits with $A, B \in SU(2)$ in Eq. (1.2). This is arguably the most fundamental notion of equivalence in quantum information theory and is known as LOCC [16, 12]. It is trace preserving, which expresses the fact that, unlike SLOCC, it is not lossy, (no state is ever discarded). Since $\dim SU(2) \times SU(2) = 6$ the LOCC equivalence classes of this 9 dimensional family of states can be represented in 3 dimensions [13]. It is remarkable that both the visualization and the interpretation of Fig. 1 remains the same when one goes from the 9 dimensional family to the 16 dimensional family of general 2 qubits states. All that changes is the notion of equivalence.

Fig. 1 turns out to play a significant role also in the theory of quantum communication. Namely, it characterizes the stochastic properties of certain *single qubit* quantum channels as shown in [21, 14, 22]. This rather different interpretation of the figure follows from a deep relation, known as the Choi-Jamiołkowski isomorphism [5], between linear operators acting on the Hilbert space of Alice and Bob, and linear maps on single qubit states. Using this, one finds, [21, 14, 22] that (for unital and trace preserving channels), the octahedron represents channels that destroy entanglement, the tetrahedron represents the completely positive maps and the cube the positive maps.

In section 3 we shall review the SLOCC interpretation of Fig. 1 from a perspective that focuses on the duality relations between the sets in the figure. The main new results concern the visualization of entanglement witnesses, duality and of the CHSH Bell inequalities in sections 4.

2 Local operations

The local mapping of a two qubit state ρ given by Eq. (1.2) preserves positivity and takes a product state $\rho_A \otimes \rho_B$ to a product state. It therefore maps any separable state—a convex combination of product states—to a separable state. This makes the equivalence $\rho \sim \rho^M$, a useful notion in studying the entanglement of two qubits [15, 26]. Since the operation does not preserve the normalization of the state it is convenient to consider states up to nor-

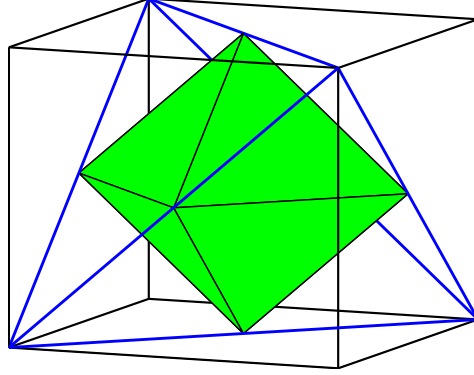


Figure 1: Three dimensional view of the world of two qubits: The cube represents the equivalence classes of potential entanglement witnesses, the tetrahedron represents the states, and the octahedron represents the separable states.

malization. The operations performed by Alice and Bob can be interpreted as *probabilistically reversible filtering* associated with the POVM

$$E_1^{(M)} = \frac{M^\dagger M}{||M||^2}, \quad E_2^{(M)} = 1 - E_1^{(M)} \quad (2.1)$$

($E_2^{(M)}$ is not a local operator. Local POVM would require four E_i 's.) The probability of successfully filtering the state $\rho^M / \text{Tr}(\rho^M)$ is strictly positive and is given by $\text{Tr}(\rho E_1^{(M)}) > 0$. When M is unitary the filtering succeeds with probability one and no state is lost. The filtering is probabilistically reversible since the original state ρ can be recovered, with non-zero probability, from ρ^M using the filter $E_1^{(M^{-1})}$.

One can broaden the notion of equivalence under SLOCC from states to observable and in particular, to witnesses W . We take the action on witnesses to be contragradient to that of states:

$$W \rightarrow W^M = (M^\dagger)^{-1} W M^{-1}, \quad M = A \otimes B, \quad A, B \in SL(2, \mathbb{C}) \quad (2.2)$$

(In case M is unitary states and observables transform the same way). The motivation for this choice is to have ρW transforms by a similarity transformation so its trace and therefore the associated expectation and probability, is left invariant.

2.1 Potential witnesses

We shall say that W_e is a *potential entanglement witness* if¹

$$\text{Tr}(W_e \rho_s) \geq 0 \quad (2.3)$$

for all separable states ρ_s . Since the set of separable states $\{\rho_s\}$ is a convex cone in the space of 4×4 matrices, the set of potential entanglement witnesses $\{W_e\}$ is the dual convex cone of $\{\rho_s\}$. The set of states, $\{\rho\}$, is a convex cone as well, and the three convex cones are evidently nested

$$\{\rho_s\} \subset \{\rho\} \subset \{W_e\} \quad (2.4)$$

The cones $\{\rho\}$, $\{\rho_s\}$ and $\{W_e\}$ all lie in 16 dimensions, which is not very useful for visualization.

SLOCC takes a potential entanglement witness to a potential entanglement witness. This follows from

$$\text{Tr}(W_e^M \rho_s) = \text{Tr}(W_e \rho_s^{M^{-1}}) \geq 0 \quad (2.5)$$

which shows that W_e^M is an entanglement witness if W_e is.

SLOCC allows one to reduce the study of states, separable states, and (potential) entanglement witnesses to the study of the corresponding equivalence classes. As will be explained in section 3, the equivalence classes of the three cones are described by the three polyhedra shown in Fig. 1.

Similar ideas can be used to visualize Bell inequalities as we now proceed to show.

2.2 Bell witnesses

Every Bell inequality has a corresponding witness [23]. Let W_B be a witness for a specific Bell inequality. A state ρ_h satisfies this Bell inequality if

$$\text{Tr}(W_B \rho_h) \geq 0 \quad (2.6)$$

Since the separable states satisfy all types of Bell inequalities [23, 12] it is clear that W_B belongs to the family of potential entanglement witnesses. The set $\{\rho\}_B$ of states satisfying (2.6) for a specific type of Bell inequalities (e.g. the CHSH family) forms a convex cone. However in general it is larger than the cone $\{\rho_s\}$ of separable states.

¹For a definition of witnesses that goes through the Choi-Jamiołkowski isomorphism, see e.g. [24].

2.3 CHSH witnesses

The CHSH Bell inequalities describe a situation where Alice may choose to measure her qubits in one of two directions, (a, a') and Bob may similarly choose one of the directions, (b, b') . It is represented by the witness [23]

$$W_B = \frac{1}{2}(2 \pm B_{CHSH}) \quad (2.7)$$

where B_{CHSH} is the CHSH operator [6]:

$$B_{CHSH}(a, a', b, b') = a \cdot \sigma \otimes (b + b') \cdot \sigma + a' \cdot \sigma \otimes (b - b') \cdot \sigma \quad (2.8)$$

$a \cdot \sigma = a_j \sigma^j$. The CHSH Bell inequality then takes the form of Eq. (2.6).

The family of all CHSH witnesses is an a-priori 8 dimensional family associated with the 4 directions Alice and Bob choose. (In fact, an implicit degeneracy in Eq. (2.8) makes it is only 7 dimensional.) LOCC takes a CHSH witness corresponding to the directions (a, a', b, b') to a witness associated with rotated directions while keeping $a \cdot a'$ and $b \cdot b'$ fixed. This reduces the dimension by 6 and allows us to visualize the equivalence classes of CHSH witnesses. As we explain in section 4, they turn out to be the three circles shown in Fig. 3.

2.4 Bell inequalities and SLOCC

Local operations, Eq. (1.2), are guaranteed to take separable states to separable states. This reflects the fact that no entangled state can ever be (locally) filtered from a separable state. This is not the case for states that satisfy Bell inequalities. In fact, [9] gave examples of states satisfying all the CHSH inequalities whose filtration violate the inequality. This is consistent because the positivity of $Tr(W_B \rho_h)$ *does not* imply positivity of $Tr(W_B \rho_h^M)$. SLOCC does not act nicely on CHSH. This can also be seen from the fact that the family of CHSH witnesses *is not* mapped on itself by SLOCC. It is therefore *not possible* to represent the states that satisfy CHSH inequalities in terms of their SLOCC equivalence classes.

It seems clear however that if a state ρ^M , filtered from ρ (using only local operations), breaks a certain Bell inequality then the properties of ρ itself are inconsistent with (more general) local hidden variables. Indeed if ρ would have been describable in terms of hidden variables that would have implied that the results of any experiment done on it including one involving

local filtration (which is also a type of measurement) should be explainable in terms of these hidden variables².

This motivates the introduction of a notion of states that satisfy Bell inequality in a SLOCC sense by requiring not only the state ρ_h satisfy the Bell inequality W_B , but also that all states that can be *probabilistically filtered* from ρ_h do. This is clearly a SLOCC invariant notion. Mathematically, it is expressed by the requirement

$$\inf_M \text{Tr}(W_B \rho_h^M) \geq 0 \quad (2.9)$$

We shall denote this set $\{\rho\}_B^{\text{SLOCC}}$. It is, of course, a smaller set, $\{\rho\}_B^{\text{SLOCC}} \subset \{\rho\}_B$, but it is not empty. This set is SLOCC invariant and so visualized in three dimensions. The corresponding 3-dimensional set is the intersection of 3 cylinders shown in Fig. 4, as we shall explain in section 4. For any fixed witness W_B the equivalence class $\{\rho\}_B^{\text{SLOCC}}$ is a convex cone since

$$\inf_M \text{Tr}(W_B(\rho_1 + \rho_2)^M) \geq \inf_M \text{Tr}(W_B \rho_1^M) + \inf_M \text{Tr}(W_B \rho_2^M) \quad (2.10)$$

Since the intersection of convex cones is a convex cone, it follows that the states that satisfy a *family* of Bell inequalities in the SLOCC sense also form a convex cone. In particular, this is so for the CHSH family. The intersection of the cone with the hyperplane $\text{Tr} \rho = 1$ is then evidently a convex set.

Similarly, the dual (convex) cone to $\{\rho\}_B^{\text{SLOCC}}$ is SLOCC invariant by Eq. (2.5), i.e. if W_B is a witness for a given SLOCC family, so is W_B^M . These notions of witnesses and states conform to the notion of SLOCC. They can therefore be represented in terms of their equivalence classes and can be visualized in three dimensions.

3 Lorentz Geometry of Two Qubits

To describe the SLOCC equivalence classes of qubits it is convenient to use their Lorentz description. Any single qubit observable Q can be written as

$$Q = q_\mu \sigma^\mu \quad (3.1)$$

²It turns out the combined experiment done on ρ consisting of filtration plus subsequent spin measurement can be described using hidden variables only if the choice of Alice whether to measure a or a' can influence the result of the filtration which was completed prior to it. This breaks natural causality assumptions. The fact that ρ does not itself break Bell's inequality may then be traced to the fact that the standard derivation of Bell's inequalities does not involve these causality assumptions.

The observable Q is then represented by the real 4-vector q .

Q is positive, and so is a state, if its trace and determinant are positive. Since $\text{Tr}Q = 2q_0 > 0$ and $\det Q = q_\mu q^\mu \geq 0$, states are described by 4-vectors q that lie in the forward light-cone. Consider

$$Q^M = MQM^\dagger = q_\mu (M\sigma^\mu M^\dagger), \quad M \in SL(2, \mathbb{C}) \quad (3.2)$$

Since $q_\mu q^\mu = \det Q = \det Q^M$, it follows that the action of $M \in SL(2, \mathbb{C})$ on the observable Q can be implemented by an (orthochronous) Lorentz transformation of the four vector q . Namely, [25],

$$Q^M = q_\mu (M\sigma^\mu M^\dagger) = (\Lambda_M q)_\mu \sigma^\mu, \quad \Lambda_M \in SO_+(1, 3) \quad (3.3)$$

Similarly, any observable W in the world of 2 qubits can be represented by by a 4×4 real matrix ω as in Eq. (1.1). This representation allows a simple geometric characterization of potential entanglement witnesses in terms of matrices ω that map the forward light-cone into itself. This follows from the fact that W is an entanglement witness iff for any product state, represented by time-like vectors ρ_a, ρ_b :

$$\text{Tr}(W\rho_a \otimes \rho_b) = 4\omega_{\mu\nu}\rho_a^\mu \rho_b^\nu = 4\rho_a^\mu (\omega\rho_b)_\mu \geq 0 \quad (3.4)$$

This characterization of potential witnesses will play a role in what follows.

To describe the SLOCC equivalence classes we shall consider invariants under the action (1.2). The pair $A, B \in SL(2, \mathbb{C})$ associated with $M = A \otimes B$ gives rise to a pair of Lorentz transformations Λ_A and Λ_B such that [26]:

$$\omega^M = \Lambda_A \omega \Lambda_B^T \quad (3.5)$$

Since $\det \Lambda_A = \det \Lambda_B = 1$, $\det \omega$ is an invariant.

A more interesting and powerful invariant is constructed as follows: The Minkowski adjoint of ω is defined as:

$$\omega^\star = \eta \omega^T \eta \quad (3.6)$$

where η is the Minkowski metric tensor. ω^\star transforms contragradiently to ω under M . This follows easily from the defining relations of the Lorentz transformation $\Lambda \eta \Lambda^T = \eta$:

$$\begin{aligned} (\omega^M)^\star &= \eta (\omega^M)^T \eta \\ &= \eta (\Lambda_A \omega \Lambda_B^T)^T \eta \\ &= (\eta \Lambda_B \eta) (\eta \omega^T \eta) (\eta \Lambda_A^T \eta) \\ &= (\Lambda_B^T)^{-1} \omega^\star (\Lambda_A)^{-1} \end{aligned} \quad (3.7)$$

It follows that $\omega^*\omega$ undergoes a similarity transformation under the action of M , so its spectrum is a SLOCC invariant.

For a general observable, $\omega^*\omega$ is not guaranteed to be a hermitian matrix, and its spectrum therefore may not be real. However, if W is a potential entanglement witness, a simplification occurs. In particular, the eigenvalues of $\omega^*\omega$ are guaranteed to be positive [26, 15]. This can be seen from the following argument: Suppose W is a *strict* witness of entanglement, so that Eq. (3.4) holds with strict inequality. $\omega^*\omega$ then maps the forward light-cone into its interior, since for any causal vector ρ

$$0 < (\omega\rho)_\mu(\omega\rho)^\mu = \rho_\mu(\omega^*\omega\rho)^\mu \quad (3.8)$$

This implies, by a fixed point argument, that the largest eigenvalue of $\omega^*\omega$ is positive and has a time-like eigenvector. The Lorentz orthogonal subspace to this eigenvector is a space-like invariant subspace. Restricted to this subspace, the Minkowsky adjoint coincides with the ordinary adjoint. This makes the remaining eigenvalues positive as well³.

Up to sign the *Lorentz singular values* [26] are defined as the roots of the eigenvalues of $\omega^*\omega$. We denote them by ω_α . They are the Lorentz analog of the singular values of a matrix⁴. As the above argument shows the largest singular value which will be denoted ω_0 corresponds generically to a timelike eigenvector (and in degenerate cases to a null one) while $\omega_1, \omega_2, \omega_3$ generically correspond to a spacelike eigenvector (or possibly a null one in degenerate cases).

Defining ω_α as the square roots of the (necessarily positive) eigenvalues of $\omega^*\omega$ still leaves a sign ambiguity. A unique determination ω_α is achieved by letting ω_3 take the sign of $\det \omega$ and choosing all others non-negative. Furthermore, one orders them according to

$$\omega_0 \geq \omega_1 \geq \omega_2 \geq |\omega_3|, \quad \text{sign}(\omega_3) = \text{sign}(\det \omega) \quad (3.9)$$

Unless ω_0 happens to vanish the SLOCC equivalence class may be characterized, up to scaling, by the three vector

$$\vec{\omega} = \frac{1}{\omega_0}(\omega_1, \omega_2, \omega_3) \quad (3.10)$$

³If one replaces $<$ by \leq above then it might happen that the largest eigenvalue has an eigenvector which is light-like. This case is much more complicated, but for our aims here can be handled by a limiting argument.

⁴ ω_α are not the covariant components of a Lorenzian 4-vector.

The SLOCC equivalence classes of potential entanglement witnesses would then be represented by the pyramid

$$\{(x, y, \pm z) \mid x \geq y \geq z \geq 0\} \quad (3.11)$$

Remarks:

- If W is a strict potential witness (implying $\omega_0 > |\omega_i|$) then it turns out [1] that in analogy to the usual singular value decomposition one can find a pair of Lorentz transformations that bring ω to its canonical form

$$\sum \omega_\alpha \sigma^\alpha \otimes \sigma^\alpha \quad (3.12)$$

This in turn imply that the singular values ω_α completely determine W 's SLOCC equivalence class.

- However if $\omega_0 = \max(|\omega_i|)$ (corresponding to a non-strict potential witness) then there is no a-priori guarantee that such a pair of Lorentz transformations exist. Witnesses W associated with this boundary case split into nonequivalent classes: those having the canonical form (3.12) and others having more complicated canonical forms [26]. Thus in the boundary case ω_α do not completely determine the SLOCC equivalence class.

Note that the condition $\omega_0 \geq |\omega_1|, |\omega_2|, |\omega_3|$ is enough to guarantee that $\omega = \text{diag}(\omega_0, \omega_1, \omega_2, \omega_3)$ takes the forward light-cone to itself and hence to guarantee that a potential entanglement witness $W = \sum \omega_\alpha \sigma^\alpha \otimes \sigma^\alpha$ having ω_α as singular values exists.

Operators $W = \sum \omega_\alpha \sigma^\alpha \otimes \sigma^\alpha$ which differ by permutation of $\omega_1, \omega_2, \omega_3$ or by flipping a sign of a pair of ω_i 's are SLOCC equivalent. There are 24 such operations corresponding to the tetrahedral group. Strictly, therefore, the SLOCC equivalence classes of W are represented by the pyramid of (3.9). However for the purpose of drawing pictures it is more aesthetic to symmetrize and give up (3.9). Now each (generic) equivalence class is represented by 24 points in the ω_i 's space(3.10). In particular, the potential entanglement witnesses are then represented by the unit cube.

3.1 SLOCC and duality

The following fact [1] allows one to translate the duality relation between potential witnesses and separable state from 16 dimensions to 3:

Theorem 1. *Let W and W' be two potential entanglement witnesses. Then:*

$$\inf_{M,N} \text{Tr}(W^N W'^M) = 4(\omega_0\omega'_0 - \omega_1\omega'_1 - \omega_2\omega'_2 + \omega_3\omega'_3) \quad (3.13)$$

where ω_α and ω'_α are the Lorentz singular values of W and W' respectively, ordered according to Eq. (3.9).

From a geometric point of view it may be more aesthetic to use an equivalent formulation of the theorem which allows using any of the 24 possible representatives ω_α (not necessarily satisfying (3.9)). This is easily achieved by replacing the r.h.s. of Eq. (3.13) by

$$4 \min \{\omega_0\omega'_0 + \omega_1\omega'_1 + \omega_2\omega'_2 + \omega_3\omega'_3\}$$

where the minimum is taken over the 24 possible representatives ω'_α .

In particular, given a potential witness W and a separable state ρ_s , we have for any representatives as in Eq. (3.10), $\vec{\omega}$ and $\vec{\rho}$, the inequality

$$0 \leq 4(1 + \vec{\omega} \cdot \vec{\rho}) \quad (3.14)$$

Fig. 3.1 demonstrates this inequality for a particular choice of W .

Since the positivity of the right hand side is the standard duality relation between convex sets in 3 dimensions [20] we see that the theorem translates the duality, Eq. (2.3), between the 16 dimensional cones, to the duality between convex sets in 3 dimensions [20].

Letting the tetrahedral group act on the pyramid of Eq. (3.11) gives the unit cube. Since the cube is the dual (also known as Polar [20]) of the octahedron one learns from Eq. (3.14) that the SLOCC equivalence classes of the separable states are represented by the octahedron (up to the tetrahedral symmetries).

The 16 dimensional set of states is self-dual. By Eq. (3.14) the corresponding SLOCC equivalence classes must be represented by a self-dual convex set in three dimensions, which turns out to be the tetrahedron. To see this note that an operator ρ in the canonical form, Eq. (3.12), is a sum of mutually commuting operators with one relation, $(\prod \sigma^\mu \otimes \sigma^\mu = -1)$. It follows that its eigenvalues are

$$\{\rho_0 + \epsilon_1\rho_1 + \epsilon_2\rho_2 - \epsilon_1\epsilon_2\rho_3\} \quad (3.15)$$

where $\epsilon_1, \epsilon_2 \in \{+1, -1\}$. Requiring ρ to be positive restricts to the intersection of four half-spaces which evidently yield the tetrahedron. This completes the derivation of Fig. 1.

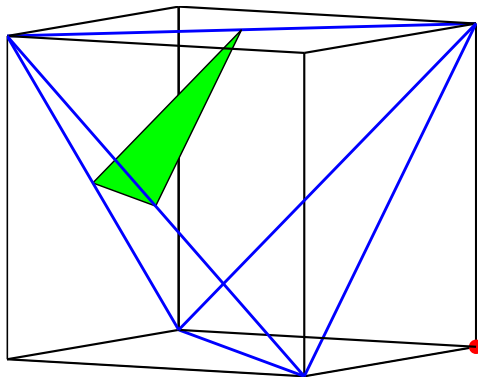


Figure 2: The red dot in the lower right corner is an entanglement witness associated with $\vec{\omega}$. The green triangle lies on the plane $\vec{\rho} \cdot \vec{\omega} = -1$. One may think of points near the corner of the tetrahedron that lie beyond the green triangle as representing the states that are incriminated as entangled by $\vec{\omega}$. The chosen witness is optimal in the sense that no other entanglement witness detects a larger set of entangled states.

One nice consequence of the geometric construction is a “proof by inspection” that for 2 qubits the Peres separability test is iff [15]. It is easy to see [18] that if ρ is a separable state, then its partial transpose is positive. The converse is not true in general, but is true for 2 qubits. However the proof [10] rests on non-elementary facts from operator algebras⁵.

The proof by inspection goes as follows [15]: Denote by ρ^P the partial transposition of ρ . Since σ_2 is antisymmetric, while the remaining σ_μ are symmetric, one has

$$(\rho^P)_{\mu\nu} = \begin{cases} -\rho_{\mu 2}, & \text{for } \nu = 2 \\ \rho_{\mu\nu}, & \text{otherwise} \end{cases} \quad (3.16)$$

On the SLOCC equivalence classes of states $\rho = \varrho_\alpha \sigma^\alpha \otimes \sigma^\alpha$, the partial transposition then acts as a reflection in the 2 axis: Replacing ϱ_2 with $-\varrho_2$. Since the octahedron of separable states is the intersection of the tetrahedron with its reflection through the $\varrho_2 = 0$ plane the result follows.

⁵See [24] for the history of this problem.

4 Visualizing the CHSH inequalities

The CHSH witnesses and inequalities were described in section 2.3. For the sake of simplicity in notation we shall now stick with the plus sign in the witness of Eq. (2.7)⁶.

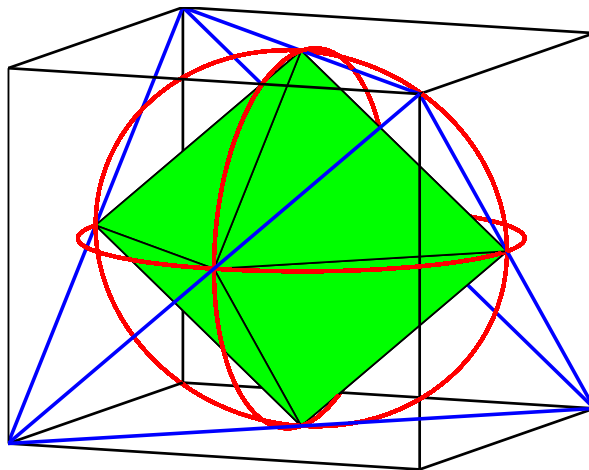


Figure 3: The circles represent the CHSH Witnesses

If a state violates a CHSH inequality then it is necessarily entangled, but the opposite claim is false; There are entangled states that do not violate any CHSH inequality. Our aim is to visualize these.

The CHSH witnesses have the property that $(\omega_B)_{0j} = (\omega_B)_{j0} = 0$. This family is invariant under the action of LOCC. The associated equivalence classes then live in three dimensions and are in 1-1 correspondence with the 3 singular values of the 3×3 matrix $\tilde{\omega}_B$

$$(\tilde{\omega}_B)_{ij} = (\omega_B)_{ij} \quad (4.1)$$

The singular values are the roots of the three eigenvalues of $\tilde{\omega}_B^\dagger \tilde{\omega}_B$.

To find the explicit dependence of the singular values on the LOCC invariants $\cos \alpha = \hat{a} \cdot \hat{a}'$ and $\cos \beta = \hat{b} \cdot \hat{b}'$ —the angles between the two directions

⁶The minus sign corresponds to flipping \hat{b}, \hat{b}' .

Alice and Bob choose—we introduce the pair of 3×2 matrices:

$$A = (\hat{a}, \hat{a}') \quad B = (\hat{b}, \hat{b}') \quad (4.2)$$

One checks that

$$2\tilde{\omega}_B = a \otimes (b + b')^T + a' \otimes (b - b')^T = A \begin{pmatrix} 1 & 1 \\ 1 & -1 \end{pmatrix} B^T \quad (4.3)$$

Since $\tilde{\omega}_B^\dagger \tilde{\omega}_B$ is manifestly a 3×3 matrix with rank 2, one of its eigenvalues is zero. Its remaining nonzero eigenvalues equal to those of the 2×2 matrix

$$\frac{1}{4}(B^T B) \begin{pmatrix} 1 & 1 \\ 1 & -1 \end{pmatrix} (A^T A) \begin{pmatrix} 1 & 1 \\ 1 & -1 \end{pmatrix} \quad (4.4)$$

Evidently

$$A^T A = \begin{pmatrix} 1 & \cos \alpha \\ \cos \alpha & 1 \end{pmatrix}, \quad B^T B = \begin{pmatrix} 1 & \cos \beta \\ \cos \beta & 1 \end{pmatrix} \quad (4.5)$$

The matrix in Eq. (4.4) now takes the form

$$\begin{pmatrix} \cos^2(\frac{\alpha}{2}) & \cos \beta \sin^2(\frac{\alpha}{2}) \\ \cos \beta \cos^2(\frac{\alpha}{2}) & \sin^2(\frac{\alpha}{2}) \end{pmatrix} \quad (4.6)$$

It has a unit trace, so the singular values of $\tilde{\omega}_B$ lie on the unit circle $\omega_1^2 + \omega_2^2 = 1$, $\omega_3 = 0$. Solving for the eigenvalues we find:

$$2\omega_{1,2}^2 = 1 \pm \sqrt{1 - \sin^2 \alpha \sin^2 \beta}, \quad \omega_3 = 0$$

As α and β vary from 0 to 2π this gives one eighth of the unit circle where $1 \geq \omega_1 \geq \omega_2 \geq 0$. If we adjoin to it the twenty four representatives of the same equivalence class, we get the three mutually intersecting unit circles, shown in Fig. 3, representing the LOCC equivalence classes of CHSH witnesses.

The dual set to the three unit circles (more precisely to their convex hull) then represents the LOCC equivalence classes of the states that satisfy all the CHSH inequalities⁷. To describe this geometrically, note that the dual set of the unit circle in the $x - y$ plane, for example, is the cylinder along the z axis, with a unit radius. The LOCC equivalence classes of states that satisfy all the CHSH inequalities, is the intersection of three cylinders along the x , y and z axes, with a unit radius. This set (see Figure 4) is bigger than the set of separable states represented by the octahedron.

⁷A-priori, only states with completely mixed subsystems are accommodated in a 3-D LOCC diagram. However, it is easy to see that ρ_{0j} and ρ_{j0} do not affect $Tr(\rho W_B)$.

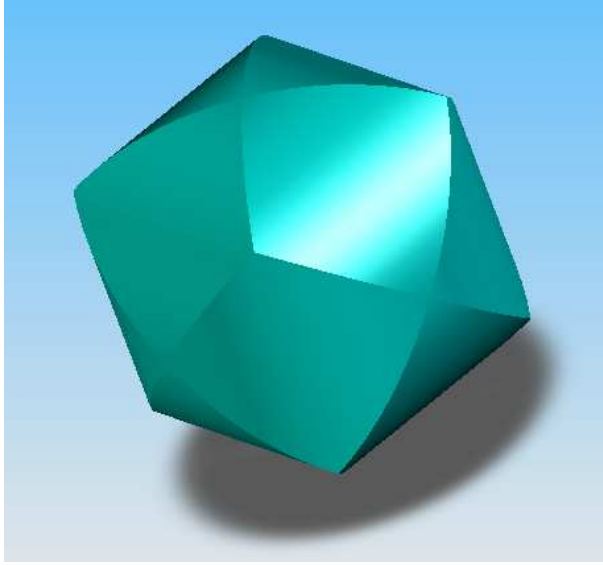


Figure 4: The set of states that satisfy all CHSH inequalities in the SLOCC sense is the intersection of three cylinders.

4.1 Optimizing the CHSH Inequality

In [11] R. Horodecki, P. Horodecki and M. Horodecki solved the problem of finding the optimal CHSH witness⁸ for a given (normalized) state ρ . They show that

$$\frac{1}{4}\text{Tr}(\rho W_B) \geq 1 - \sqrt{\rho_1^2 + \rho_2^2} \quad (4.7)$$

and the inequality is saturated for an appropriate choice of angles α, β . Here $\rho_{1,2}$ are the two largest singular values of the 3×3 matrix $\tilde{\rho}$ constructed from the spatial components of the matrix elements $\rho_{\mu\nu}$ as in Eq. (4.1). In particular, the state ρ violates a CHSH inequality if and only if $\rho_1^2 + \rho_2^2 > 1$.

This result can be derived, essentially by inspection, from the geometric description of the previous section. Recall, (see footnote 7), that the state ρ may be assumed, without loss, to be one where the subsystems are completely mixed. The LOCC equivalence class of ρ is represented by the three singular values of $\tilde{\rho}$, which we denote by $\vec{\rho}$. A Bell witness, is represented by the three singular values of $\tilde{\omega}_B$, which we denote by $\vec{\omega}_B$. The vector $\vec{\omega}_B$ takes values

⁸See also [28].

on the three circles in the figure. For a normalized state ρ

$$\frac{1}{4}\text{Tr}(\rho W_B) = 1 + \vec{\rho} \cdot \vec{\omega}_B \quad (4.8)$$

It is clear that the optimal choice of a witness (a minimizer) is to choose the witness $\tilde{\omega}_B$ so that the vector $\vec{\omega}_B$ is as anti-parallel to $\vec{\rho}$ as possible. (Recall that $\vec{\omega}_B$ is constrained to lie in one of the principle planes.) The minimizer is then smallest entry among

$$\{1 - |\vec{\rho} \times \hat{x}|, 1 - |\vec{\rho} \times \hat{y}|, 1 - |\vec{\rho} \times \hat{z}|\} \quad (4.9)$$

This reproduces the result of the Horodeckies.

4.2 SLOCC interpretation

Fig. 4 also admits the following SLOCC interpretation: The states represented by points lying in the intersection of the three cylinders have the property that they, and all that can be filtered from them, satisfy all the CHSH inequalities. This is an immediate consequence of theorem 1 which guarantees that $\text{Tr}(\rho^{A \otimes B} W_B)$ attains its minimum value when ρ takes its canonical form.

The SLOCC equivalence classes of states that lie outside the intersection of the cylinders have the property that they can always be filtered to yield states that violate some CHSH inequality.

5 More can be less

The CHSH inequality constrains Alice and Bob to two dichotomic tests each. A general theory of Bell inequalities allows Alice and Bob n_A and n_B tests, having m_A and m_B possible results. (A geometric framework for deriving such generalized Bell inequalities is described in [19].) Let $I(n_A n_B m_A m_B)$ denote a corresponding Bell inequality. The CHSH inequality is then $I(2222)$. Von Neumann tests on qubits restricts the outcomes of each test to two, $m_A = m_B = 2$, however, the number of tests, n_A, n_B can be arbitrary.

One naively expects that by increasing the number of tests one might be able to incriminate some of the entangled states that pass the CHSH test. Indeed, D. Collins and N. Gisin [7] present an example of a state ρ that violates an $I(3322)$ inequality but does not violate any CHSH inequality.

Here we shall present numerical evidence which shows that when Bell inequalities are interpreted in the SLOCC sense then $I(3322)$ (with three dichotomic tests), is strictly weaker than $I(2222)$. It follows that the state found by Collins and Gisin can be filtered to a state that violates CHSH.

The $I(3322)$ inequality derived by D. Collins and N. Gisin [7] takes the form

$$-2P(B_1) - P(B_2) - P(A_1) + P(A_1B_1) + P(A_1B_2) + P(A_1B_3) + P(A_2B_1) + P(A_2B_2) - P(A_2B_3) + P(A_3B_1) - P(A_3B_2) \leq 0$$

where $P(A_iB_j)$ is the probability that when Alice chooses the i th measurement and Bob chooses the j th measurement, they both get the outcome 0.

Allowing Alice and Bob three experiments to choose from gives them more freedom. In particular, they are always free to disconnect the third experiment. This means that the CHSH, or $I(2222)$, must be a special case of $I(3322)$. Indeed, the CHSH $I(2222)$ inequality,

$$P(A_1B_1) + P(A_1B_2) + P(A_2B_1) - P(A_2B_2) - P(B_1) - P(A_1) \leq 0$$

is obtained from $I(3322)$ by Alice disconnecting her third experiment, $P(A_3) = 0$, and Bob disconnecting his first experiment, $P(B_1) = 0$. Renaming B_2 and B_3 as B_1 and B_2 respectively gives CHSH.

Dichotomic, von Neumann, tests of Alice and Bob are described by projection operators, namely setting in the above

$$P(A_iB_j) \rightarrow \frac{1 + a_i \cdot \sigma}{2} \otimes \frac{1 + b_j \cdot \sigma}{2} \quad (5.1)$$

where a_i and b_j are interpreted as directions in a measurement of the spin projection. Note that the case of a disconnected experiment *is not* of this form: It is not a dichotomic von Neumann measurement.

The witness corresponding to $I(3322)$ with three dichotomic von Neumann measurements for both Alice and Bob is then

$$\begin{aligned} W_{3322} = & 4I \otimes I + I \otimes (b_1 + b_2) \cdot \sigma - (a_1 + a_2) \cdot \sigma \otimes I \\ & - (a_1 + a_2) \cdot \sigma \otimes (b_1 + b_2) \cdot \sigma - (a_1 - a_2) \cdot \sigma \otimes b_3 \cdot \sigma \\ & - a_3 \cdot \sigma \otimes (b_1 - b_2) \cdot \sigma \end{aligned} \quad (5.2)$$

$Tr(\rho W_{3322}) < 0$, implies that the state ρ violates a Bell inequality.

W_{3322} represents an (a-priori) 12 dimensional family of witnesses. It has six LOCC invariant parameters, the angles $\cos(\alpha_{ij}) = a_i \cdot a_j$ and $\cos(\beta_{ij}) = b_i \cdot b_j$, $i \neq j \in \{1, 2, 3\}$. We can visualize this family in 3 dimensions by representing $W_{3322} = (\omega_{3322})_{\mu\nu} \sigma^\mu \otimes \sigma^\nu$ by its canonical form under $SL(2, \mathbb{C})$.

Let us introduce the following direction matrices

$$A = \begin{pmatrix} 1 & 0 & 0 & 0 \\ 0 & a_{1x} & a_{2x} & a_{3x} \\ 0 & a_{1y} & a_{2y} & a_{3y} \\ 0 & a_{1z} & a_{2z} & a_{3z} \end{pmatrix} \quad B = \begin{pmatrix} 1 & 0 & 0 & 0 \\ 0 & b_{1x} & b_{2x} & b_{3x} \\ 0 & b_{1y} & b_{2y} & b_{3y} \\ 0 & b_{1z} & b_{2z} & b_{3z} \end{pmatrix} \quad (5.3)$$

and

$$W_0 = \begin{pmatrix} 4 & -1 & -1 & 0 \\ 1 & -1 & -1 & -1 \\ 1 & -1 & -1 & 1 \\ 0 & -1 & 1 & 0 \end{pmatrix} \quad (5.4)$$

so $\omega_{3322} = AW_0B^T$. The Lorentz singular values are the roots of the eigenvalues of $(B^T\eta B)W_0^T(A^T\eta A)W_0$. One finds

$$A^T\eta A = \begin{pmatrix} 1 & 0 & 0 & 0 \\ 0 & -1 & -\cos(\alpha_{12}) & -\cos(\alpha_{13}) \\ 0 & -\cos(\alpha_{12}) & -1 & -\cos(\alpha_{23}) \\ 0 & -\cos(\alpha_{13}) & -\cos(\alpha_{23}) & -1 \end{pmatrix} \quad (5.5)$$

$$B^T\eta B = \begin{pmatrix} 1 & 0 & 0 & 0 \\ 0 & -1 & -\cos(\beta_{12}) & -\cos(\beta_{13}) \\ 0 & -\cos(\beta_{12}) & -1 & -\cos(\beta_{23}) \\ 0 & -\cos(\beta_{13}) & -\cos(\beta_{23}) & -1 \end{pmatrix} \quad (5.6)$$

The Lorentz singular values were calculated numerically. The intersection of the resulting set with the $X - Y$ plane, shown in Fig. 5 is clearly contained in the CHSH unit circle. Similarly all points outside this plane were found to lie inside the convex hull of the three CHSH circles, implying they represent weaker witnesses. This means that under SLOCC the CHSH inequality is stronger than I_{3322} (when Alice and Bob are constrained to measure three spin directions each).

Thus, if the two parties are allowed to filter then by letting them choose from 3 possible experiments, we gain less information than by restricting them to choose from 2 possible experiments.

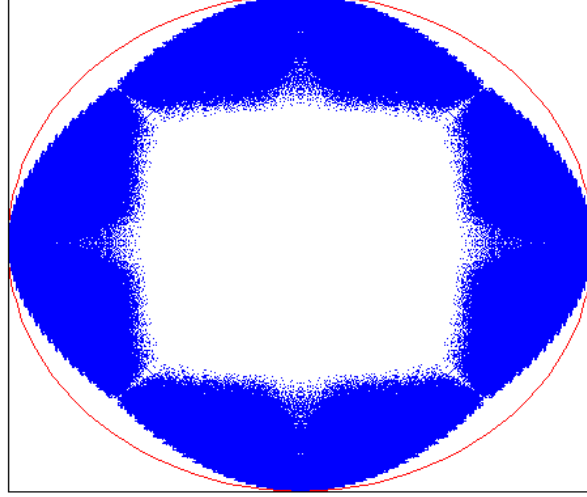


Figure 5: CHSH and I_{3322} Witnesses in the $X - Y$ plane: the circle represent CHSH witnesses while all the dots inside represent I_{3322} witnesses in this plane. Since the dots lie inside the circle they represent weaker witnesses.

6 Concluding remarks

Many of the important concepts in quantum information, such as entangled and separable states, entanglement witnesses, the CHSH Bell inequalities etc. can be visualized in three dimensions by introducing an appropriate equivalence relation. The visualization allows us to give a “proof by inspection” of the non-elementary fact [10] that the Peres separability test for 2 qubits is iff. It also allows us to “solve by inspection” the problem of optimizing the CHSH Bell inequality, which was solved by analytical methods in [11].

We have introduced the notion of states that satisfy Bell inequalities in the SLOCC sense. We gave numerical evidence which shows that allowing Alice and Bob an additional *dichotomic von Neumann* test does not enable them to shrink the set shown in Fig. 4, obtained by filtering and CHSH. It is an interesting open question whether four or more dichotomic tests, or more general POVM tests, can further shrink the set shown in Fig. 4.

Acknowledgment: This work is partially supported by the ISF. We

thank Michael Burman for his help with drawing figure 4, Netanel Lindner for discussions and Mary Beth Ruskai for a helpful correspondence and several useful suggestions.

References

- [1] J. E. Avron and O. Kenneth. in preparation.
- [2] Charles H. Bennett, Sandu Popescu, Daniel Rohrlich, John A. Smolin, and Ashish V. Thapliyal. Exact and asymptotic measures of multipartite pure-state entanglement. *Phys. Rev. A*, 63(1):012307, Dec 2000.
- [3] R. A. Bertlmann, H. Narnhofer, and W. Thirring. Geometric picture of entanglement and bell inequalities. *Phys. Rev. A*, 66(3):032319, 2002.
- [4] D Bruß. Characterizing entanglement. *J. Math. Phys.*, 43:4237, 2002, arXiv:qunat-ph/0110078.
- [5] M. D. Choi. Completely positive linear maps on complex matrices. *Lin. Alg. Appl.*, 10:285–290, 1975.
- [6] John F. Clauser, Michael A. Horne, Abner Shimony, and Richard A. Holt. Proposed experiment to test local hidden-variable theories. *Phys. Rev. Lett.*, 23(15):880–884, Oct 1969.
- [7] D. Collins and N. Gisin. A relevant two qubit bell inequality inequivalent to the chsh inequality. *Journal of Physics A: Mathematical and General*, 37:1775–1787(13), 2004.
- [8] W. Dür, G. Vidal, and J. I. Cirac. Three qubits can be entangled in two inequivalent ways. *Phys. Rev. A*, 62(6):062314, Nov 2000.
- [9] N. Gisin. Hidden quantum nonlocality revealed by local filters. *Physics Letters A*, 210:151–156(6), 1996.
- [10] M. E. Horodecki, P. Horodecki, and R. Horodecki. Separability of mixed states: necessary and sufficient conditions. *Physics Letters A*, 223(1):1–8, November 1996.

- [11] R. Horodecki, P. Horodecki, and M. Horodecki. Violating bell inequality by mixed spin-1/2 states: necessary and sufficient condition. *Physics Letters A*, 200:340–344(5), 1995.
- [12] R. Horodecki, P. Horodecki, M. E. Horodecki, and K. Horodecki. Quantum entanglement. 2007, quant-ph/0702225.
- [13] Ryszard Horodecki and Michal Horodecki. Information-theoretic aspects of inseparability of mixed states. *Phys. Rev. A*, 54(3):1838–1843, September 1996.
- [14] Chris King and Mary Beth Ruskai. Minimal entropy of states. *IEEE Trans. Info. Theory*, 47:192–209, 1999, quant-ph/9911079.
- [15] Jon Magne Leinaas, Jan Myrheim, and Eirik Ovrup. Geometrical aspects of entanglement. *Physical Review A (Atomic, Molecular, and Optical Physics)*, 74(1):012313, 2006.
- [16] Michael A. Nielsen and Isaac L. Chuang. *Quantum Computation and Quantum Information*. Cambridge U.P., 2000.
- [17] Asher Peres. *Quantum Theory: Concepts and Methods*. Springer, 1995.
- [18] Asher Peres. Separability criterion for density matrices. *Phys. Rev. Lett.*, 77(8):1413–1415, Aug 1996.
- [19] Asher Peres. All the bell inequalities. *Foundations of Physics*, 29(4):589–614, April 1999.
- [20] R. Tyrrell Rockafellar. *Convex Analysis*. Princeton University Press, 1970.
- [21] Mary Beth Ruskai. Qubit entanglement breaking channels. *Rev. Math. Phys.*, 15:643–662, 2003, quant-ph/0302032v3.
- [22] Mary Beth Ruskai, Stanislaw Szarek, and Elisabeth Werner. An analysis of completely-positive trace-preserving maps on 2x2 matrices. 2001, quant-ph/0101003v2.
- [23] B. M. Terhal. Bell inequalities and the separability criterion. *Physics Letters A*, 271(5):319–326, July 2000.

- [24] Barbara M. Terhal. Detecting quantum entanglement. *Journal of Theoretical Computer Science*, 287(1):313–335, 2002, quant-ph/0101032.
- [25] Wu-Ki Tung. *Group theory in physics*. World Scientific, 1985.
- [26] Frank Verstraete, Jeroen Dehaene, and Bart De Moor. Lorentz singular-value decomposition and its applications to pure states of three qubits. *Phys. Rev. A*, 65(3):032308, Februar 2002.
- [27] K. G. H. Vollbrecht and R. F. Werner. Entanglement measures under symmetry. *Phys. Rev. A*, 64(6):062307, 2001.
- [28] Reinhard F. Werner and Michael M. Wolf. Bell inequalities and entanglement. arXiv:quant-ph/0107093, 2001.